

STRING POTENTIOMETER BLADE MOTION MEASUREMENT SYSTEM APPLIED TO FULLY ARTICULATED INTER-BLADE ROTOR

Marco Dornetti

Engineer, Structural Dynamics Dept. (AW)

marco.dornetti@agustawestland.com

Ermanno Fosco

Senior Engineer, Structural Dynamics Dept. (AW)

ermanno.fosco@agustawestland.com

Giovanni Facchini

Chief Project Engineer, Rotor RSD&D Dept (AW).

giovanni.facchini@agustawestland.com

Alberto Angelo Trezzini

Engineer, Structural Dynamics Dept. (AW)

albertoangelo.trezzini@agustawestland.com

Attilio Colombo

Head of Structural Dynamics Dept. (AW)

attilio.colombo@agustawestland.com

Giuseppe Piccirillo

Engineer, Ground Support Equipment (PTA).

piccirillo.pta@agustawestland.com

Abstract

Innovations in design represent an essential ingredient to continuously improve performances and reliability of flying products.

In particular, the competitiveness of a helicopter is directly related to the efficiency of its rotors, which determine performances, loads and comfort for the entire aircraft and its occupants.

The architecture of the rotor and its behavior in flight are important ingredients to be investigated in order to obtain the best compromise in terms of market attractiveness and engineering feasibility; on this subject, one of the key factors in the development and evaluation of a rotor system is the knowledge of in-flight blade motions, which is a task that historically required significant engineering effort in order to get accurate and reliable measurements.

Present paper describes the application of a new concept of blade motion measurement system applied to a recently developed main rotor inter-blade architecture, which employs rotational dampers fitted in the tension links of the corresponding blades and connected also to the following blades by means of metallic links.

The requirements at the basis of the development of a new measurement system are the need of very compact equipment, compatible with the limited space available on the new hub architecture, together with reliability improvements with respect to existing devices.

In general, the importance of such a system is to allow the reconstruction of the rotor motion providing pitch, flap and lag angles time histories of the blade; these data are then used basically to correlate with flight mechanics models, compare with rotor loads scenario and provide on-field measurements helping in the life definition of elastomeric components.

In this paper we deal with all the system stages, starting from the early hardware design and development activity, through dedicated software implementation, up to the final phases of system calibration, flight data processing and correlation.

As far as hardware design, measurements on new inter-blade rotor architecture cannot be managed as for hub-to-blade solution, which used damper motion as input for the kinematics computation; in fact, in the inter-blade architecture, being the damper connected to two consequent blades, it doesn't provide information about absolute position of the blade. Moreover, the absence of the damper attachment point on the hub makes difficult to fit an analogous mechanical system, consisting of angular potentiometers fitted on a crank connected-rod mechanism.

For these reasons, a more compacted measurement technology based on string potentiometers sensors has been adopted, helping both in terms of ease of installation and system flexibility.

In fact, string potentiometers can be easily installed on the rotor and cable path can be simply managed in terms of optimal position in order to guarantee both measurement effectiveness and clearance with all the moving parts of the rotor.

The adopted measurement system configuration is made of three sensors for each blade: potentiometer bodies are installed on the tension link through a removable plate, whereas cables are linked to the hub by means of a dedicated support, providing blade positioning with respect to the hub itself.

The final location of the attachment points, both on the blade and hub sides, is the result of a detailed evaluation assessment, carried out with the aim of finding the optimum between measurements accuracy and motions decoupling (in terms of flap, lag and pitch degrees of freedom), within mechanical clearance constraints.

This work has been performed starting from CATIA environment and developing a multi-body model to analyze in depth kinematics and support the design phase; in parallel, an in-house Matlab code has been developed and validated with previous models, in order to manage design sensitivity analyses and provide a valid tool to process flight data on the prototypes.

Starting from the six string potentiometers signal, mentioned code allows basically the reconstruction of the time histories related to the angles of two consecutive blades; using these results and modeling the kinematics of the inter-blade rotor architecture as rigid, computation of damper angle and full set of damper link rod-end rotations have been provided.

Once calibrated, this system flew for over 100 flight hours without technical issues and providing high accuracy of its measures. Moreover, the good reconstruction of damper motions starting from measurements on two consecutive blades can be considered a significant achievement, validating the entire process and providing a solid basis to infer rod-end rotations from the reconstructed kinematics.

The new system can be easily tailored on other rotors and different architectures, with minimum design impact and optimization effort.

1 INTRODUCTION

Helicopter performances represent a set of key parameters that contribute to determine technical competitiveness and market attractiveness of such a product.

On that respect, the efficiency achieved by its rotors is essential to guarantee a competitive level of performances, loads and comfort for the entire aircraft and its occupants.

Design, development and evaluation of a rotor system take benefit from a detailed knowledge of in-flight blade motions, therefore highlighting the importance of dedicated measurements on these primary components.

This task historically required significant engineering effort in order to set-up an effective measurement system, able to guarantee accurate and reliable data collection.

This paper describes the application of a new concept of blade motion measurement system applied to a recently developed main rotor inter-blade architecture, where compactness and reliability are essential design parameters.

String potentiometer sensors have been selected in order to enhance installation easiness and flexibility as well as complying with compactness requirements.

In fact, the employment of traditional technology based on angular potentiometers and mechanical connection elements was discarded after preliminary evaluations, because of incompatibility with the new rotor architecture.

The following paragraphs will go through all the measurement system stages starting from the early hardware design and development activity, through dedicated software implementation, up to the final

phases of system calibration, flight data processing and correlation.

Results about blade pitch, lag and flap angle reconstructions are provided in terms of time histories at two consecutive blades; in addition, a rigid modeling of the rotor inter-blade kinematics and the subsequent process validation in terms of damper rotation, both measured in flight and analytically reconstructed, is presented.

Starting from these intermediate results, which provide a solid basis to extend the investigation about rotor in-flight dynamic behavior, the attention moved on the evaluation of the damper link rod-end rotations, which are essential to determine the life of elastomeric components, despite the absence of dedicated direct measurements.

The interest about this new concept of measurement system could be enhanced from the possibility to easily retrofit this installation on existing rotors, as well as tailoring it with small modifications for future applications; on that respect, this paper highlights possible improvements, especially on the calibration procedures, that could represent the core of a future continuation work.

2 TECHNICAL REQUIREMENTS AND TARGET

The installation of angular potentiometers and related mechanical interfaces, which represented the state of the art in terms of instrumentation layout for blade motion reconstruction in rotors articulated architecture, has been considered inadequate for inter-blade configuration.

The technical reasons at the basis of this incompatibility are the absence of a damper attachment structure on the hub, which was traditionally employed as hard point to support the instrumentation assembly, as well as the need of an additional sensor in place of the damper stroke

measurement, which no more represents an independent parameter in the inter-blade architecture.

Moreover, the new constraints in terms of available room emphasized the criticality of fitting an additional potentiometer and got even more challenging the compliance to the tight clearance requirements derived from proximity of a number of movable rotor components.

In parallel to the boundaries described so far, the target of this new measurement solution was defined as a compromise of the following technical/functional aspects:

- ✓ provide simple but reliable installation set-up;
- ✓ limit acquisition and maintenance costs;
- ✓ improve measurement accuracy, with particular focus on possible functional degradation over time.

This last point is the expression of the requirements directed to build up a system able to support all the development/certification activity, in place of just providing results during dedicated flight activities that usually is a limited number of flights. In other words, the purpose of this system is not only to provide angles measurements for some specific flights but also to provide rotor motions along many hours of flights and to allow studying some dynamic phenomena typical of helicopter, such as for example ground and air resonance.

3 ARCHITECTURE AND LAYOUT OPTIMIZATION

On the lights of previous remarks, particular effort has been spent in order to find the more compact solution to be fitted in the small available room. In this context, the choice about cable position transducers helps both in terms of installation compactness and system flexibility, being the cable employment easier than the corresponding connecting rods of previous standard installation. Moreover, the analysis about the clearances between cables and rotating parts, time expensive because of the rotor inter-blade architecture, becomes less critical by using string potentiometer.

The first proposed sensors configuration is reported in the Figure 1. It can be observed that all the 3 transducer bodies are located directly on the pitch lever, because of the very restricted room available on the hub, as mentioned before. Then, each sensor cable is linked to a dedicated support installed on the hub, in order to provide a measure of the blade positioning with respect to the hub itself.

The installation of the string potentiometers on the tension link together with the position of their connections to the hub has been iteratively found with an optimization process.

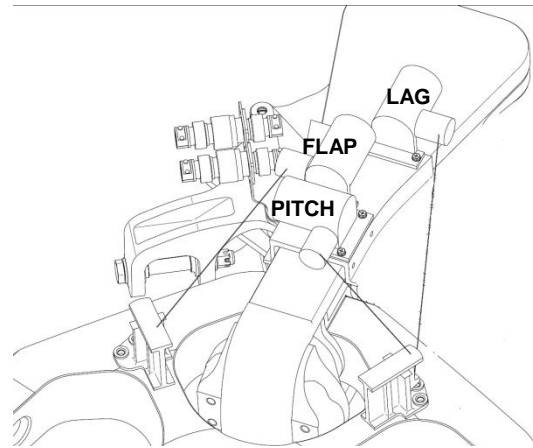


Figure 1 – First proposed configuration

In order to fulfill all the constraints both in terms of available space and clearances with all the moveable parts, an optimization process of the layout has been done starting from CATIA environment for clearance study and through a ADAMS multibody model for the kinematics optimization. Scope of this optimization process was to guarantee clearance with respect to other moving parts of the rotor and to find the optimum between measurements accuracy and motions decoupling (in terms of flap, lag and pitch degrees of freedom). In parallel to CATIA and ADAMS model, an in-house Matlab code has been developed and validated with previous models in order perform sensitivity analyses (as for example improve de-coupling between measurement and angle motions) and provide a valid tool to process flight data on the prototypes. After this optimization procedure, the first solution reported in Figure 1 was superseded by a second one, with the goal of reducing the coupling between pitch angle and lead-lag sensor readout. The solution found requires a rotated installation of the lead-lag transducer on the tension link itself with respect to solution 1. The proposed alternative solution is reported in Figure 2.

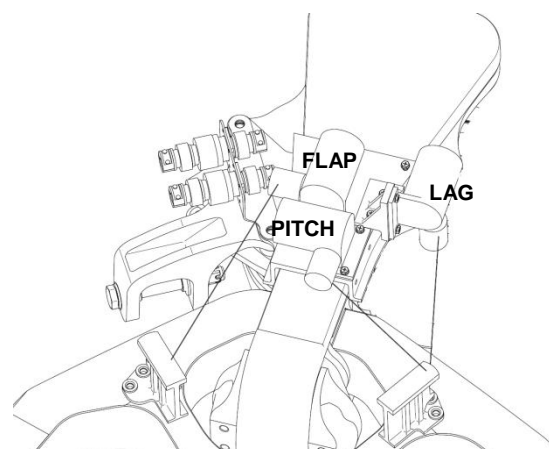


Figure 2 - Second proposed configuration

The designed system is made of three string potentiometers installed on the tension link of two subsequent blades: these potentiometers (not yet installed on the rotor) are shown in the following Figure 3. When installed in the tension link, the cables are connected in specific positions on the hub which is considered the reference fixed frame.

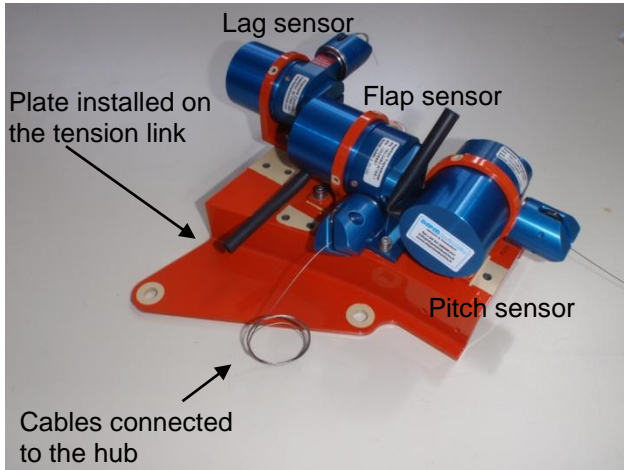


Figure 3 – String potentiometer installed on the dedicated plate (related to the first solution)

The layout shown in Figure 3 is related to the first layout proposed; the final layout installed on the rotor after the optimization has the lead-lag sensor rotation of 90°.

The readouts of the potentiometers is measured during flight and, processed by means of an in-house Matlab code, produces the time histories of in-flight blade motions (lead-lag, flap and pitch). The following paragraphs describe the final configuration of the system, the equations employed to solve the kinematic problem, the installation and calibration of the system and the validation in flight.

4 FINAL DESCRIPTION OF THE SYSTEM

The sensors configuration is reported in Figure 4, where it can be observed that all the 3 transducer bodies are located directly on the tension link lever, because of the very restricted room available on the hub, as mentioned before. The installation of the potentiometers is managed by a unique plate, which has the function of interface with the pitch lever bolts, without any contact with the tension link; this suspended connection guarantees the free deformation of the tension link during flight.

Each sensor cable is attached to a dedicated support installed on the hub, in order to provide a measure of the blade positioning with respect to the hub itself.

In Figure 5 the cable potentiometer is shown; on the right it is also visible the RoundAbout™ cable guide component mounted on the potentiometer body (in

the figure, the red line shows its axis of rotation), which has the function of allowing large cable rotation in the 2 orthogonal planes containing the nominal axis.

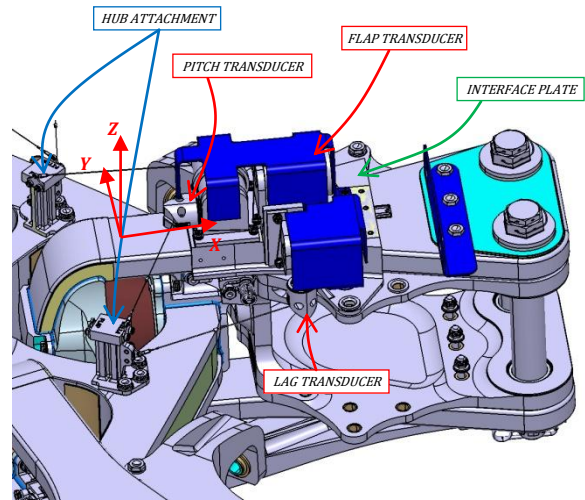


Figure 4 – System installation detail

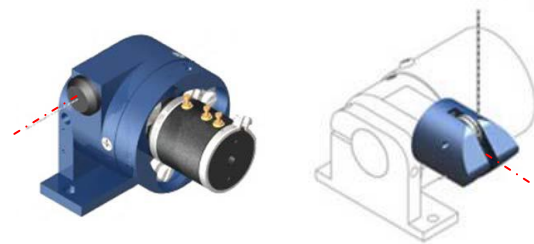


Figure 5 – Miniature cable position transducer

The main characteristics related to this model of transducer are resumed in the following table.

Table 1 – Transducer characteristics

Supplier	Firstmark Controls
Transducer Model	P/N 160-0483-R7SS
Overall stroke	152 mm
Cable tension	8-20 N
Weight	113 g
Dimension envelope	64.01 x 55.63 mm

The measures of the three potentiometers (for each instrumented blade) allow the evaluation of the lag, flap and pitch blade angles through a set of equations that is presented in the next section.

4.1 Blade angle reconstruction

In Figure 6 a scheme of the blade angles reconstruction system is depicted, for the sake of clarity, only the pitch transducer is displayed.

Figure 7 show the top view of the transducer schematized with the two pulleys belonging to the roundabout.

The cable is attached to the hub (\vec{X}_H) on one end and rolled on the pulley on the other. The roundabout is free to rotate around its axes (red dotted line) and its position is such that the medium plane of the pulley contains the hub cable attachment. It follows that the cable, during the blade movements, belongs to the aforementioned plane.

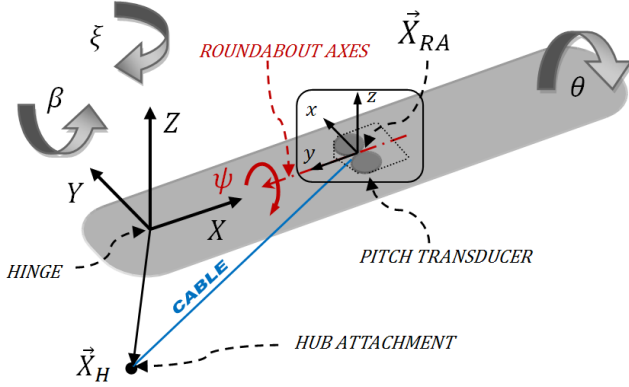


Figure 6: System scheme

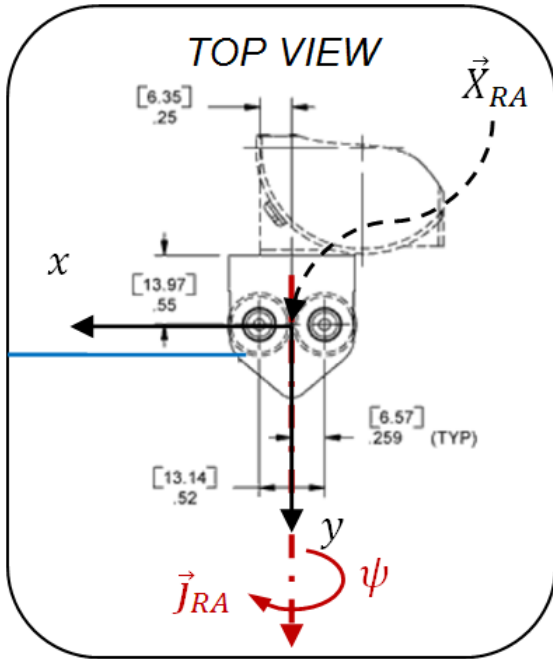


Figure 7 – System scheme – TOP VIEW

The blade angles are lag, flap and pitch (ξ, β, θ), the roundabout angle is called ψ . In Figure 8 a particular of the plane containing the cable, the pulley and the hub attachment point is shown.

\vec{X}_{RA} is the pulleys centre with regard to a fixed reference system (attached to the hub, centered at the blade hinge). \vec{X}_C is the centre of the pulley, \vec{X}_T is the tangency point of the cable on the pulley, \vec{X}_E is

the position of the cable end and \vec{X}_H is the cable position attachment on the hub.

The equations (one for each transducer) can be written imposing the matching between the position of the cable end and the cable attachment on the hub:

$$\vec{X}_H = \vec{X}_E \quad \text{Eq. 4-1}$$

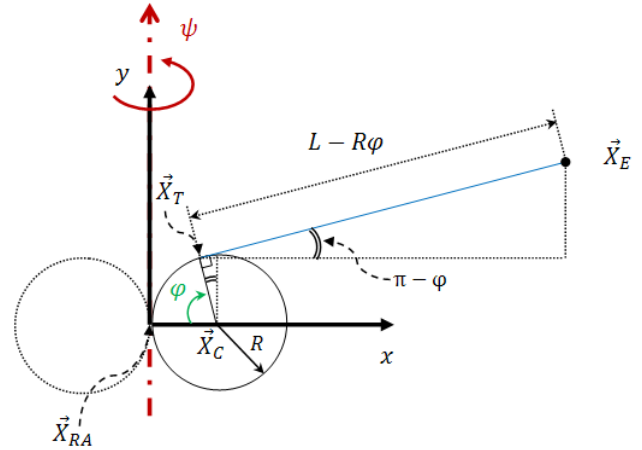


Figure 8: Detail of the system scheme

The positions can be written in terms of the unrotated positions (i.e. $\xi = \beta = \theta = 0^\circ$) and of the blade angles. Being \vec{X}_{RA}^* the unrotated position* of the roundabout centre, the position of the cable end \vec{X}_E can be expressed as:

$$\vec{X}_E = \mathcal{R}_{BLADE} \vec{X}_{RA}^* + \mathcal{R}_{RA} (\mathcal{R}_{BLADE} (\vec{X}_E^* - \vec{X}_{RA}^*)) \quad \text{Eq. 4-2}$$

Where \mathcal{R}_{BLADE} is the blade matrix of rotation, considering the blade angle rotation sequence ξ, β, θ ; \mathcal{R}_{RA} is the matrix that describes the rotation of the pulleys with respect to the roundabout axes. \vec{X}_{RA}^* is the pulleys centre, \vec{X}_E^* is the position of the cable end.

\mathcal{R}_{BLADE} can be expressed as function of ξ, β, θ as follows:

$$\mathcal{R}_{BLADE}(\xi, \beta, \theta) = [\mathcal{R}(\xi)]^T [\mathcal{R}(\beta)]^T [\mathcal{R}(\theta)]^T = \quad \text{Eq. 4-3}$$

$$= \begin{bmatrix} \cos(\xi) & \sin(\xi) & 0 \\ -\sin(\xi) & \cos(\xi) & 0 \\ 0 & 0 & 1 \end{bmatrix}^T \begin{bmatrix} \cos(\beta) & 0 & -\sin(\beta) \\ 0 & 1 & 0 \\ \sin(\beta) & 0 & \cos(\beta) \end{bmatrix}^T \begin{bmatrix} 1 & 0 \\ 0 & \cos(\theta) & \sin(\theta) \\ 0 & -\sin(\theta) & \cos(\theta) \end{bmatrix}^T$$

The expression of the rotation matrix of the pulley is obtained thanks to the Euler-Rodrigues formula, which describes the rotation of a vector given an axis of rotation and an angle of rotation:

$$\mathcal{R}_{RA}(\psi, \vec{j}_{RA}) = [I] + \sin(\psi) [\vec{j}_{RA \times}] + (1 - \cos(\psi)) [\vec{j}_{RA \times}] [\vec{j}_{RA \times}] \quad \text{Eq. 4-4}$$

* In the following, the unrotated positions are indicated with the superscript *

\vec{j}_{RA} is the unit vector that represents the roundabout axes around which the pulley rotation takes place, ψ is the amplitude of rotation. The matrix $[j_{RA \times}]$, represents the vector cross product and is defined as follows:

$$[j_{RA \times}] = \begin{bmatrix} 0 & -\vec{j}_{RA}(3) & \vec{j}_{RA}(2) \\ \vec{j}_{RA}(3) & 0 & -\vec{j}_{RA}(1) \\ -\vec{j}_{RA}(2) & \vec{j}_{RA}(1) & 0 \end{bmatrix} \quad \text{Eq. 4-5}$$

\vec{j}_{RA} is the vector that represents the rotated roundabout axes that can be obtained from the unrotated vector \vec{j}_{RA}^* as follows:

$$\vec{j}_{RA} = \mathcal{R}_{BLADE} \vec{j}_{RA}^* \quad \text{Eq. 4-6}$$

Finally (see Figure 8) it is possible to write the position of the cable end with respect to the pulleys centre ($\vec{X}_E^* - \vec{X}_{RA}^*$) as:

$$\vec{X}_E^* - \vec{X}_{RA}^* = (\vec{X}_C^* - \vec{X}_{RA}^*) + (\vec{X}_T^* - \vec{X}_C^*) + (\vec{X}_E^* - \vec{X}_T^*) \quad \text{Eq. 4-7}$$

This expression is function of the angle φ that measures the unrolling of the cable on the pulley and the cable length L (L is the length of the cable from \vec{X}_{RA}^* to \vec{X}_E^*). For example in the case of the pitch transducer:

$$\begin{aligned} \vec{X}_C^* - \vec{X}_{RA}^* &= \begin{Bmatrix} -R \\ 0 \\ 0 \end{Bmatrix} \\ \vec{X}_T^* - \vec{X}_C^* &= \begin{Bmatrix} -(L - R\varphi) \sin \varphi \\ +(L - R\varphi) \cos \varphi \\ 0 \end{Bmatrix} \\ \vec{X}_E^* - \vec{X}_T^* &= \begin{Bmatrix} -(R \cos \varphi) \\ R \sin \varphi \\ 0 \end{Bmatrix} \end{aligned} \quad \text{Eq. 4-8}$$

where R is the radius of the pulley. Writing Eq. 4-1 for the three transducers and using the ingredients detailed above, a square 9x9 system of nonlinear implicit equations is obtained:

$$\vec{\phi}(\xi, \beta, \theta, \psi_\xi, \psi_\beta, \psi_\theta, \varphi_\xi, \varphi_\beta, \varphi_\theta; L_\xi, L_\beta, L_\theta) = 0 \quad \text{Eq. 4-9}$$

The solution of this equation, via numerical iteration, provides the three blade angles (ξ, β, θ).

It also provides the three pulley rotations (one for each potentiometer) about the roundabout axis ($\psi_\xi, \psi_\beta, \psi_\theta$) and the three angles of cable unrolling on the pulley ($\varphi_\xi, \varphi_\beta, \varphi_\theta$).

The cable lengths L_ξ, L_β, L_θ are known, depending on the transducer measures.

4.2 In-house Matlab code description

The congruence equations (Eq. 4-1) for the three transducers give rise to a 9x9 system of non linear equations $\vec{\phi}$ (Eq. 4-9). This equation depends upon two sets of parameters: geometrical quantities (\vec{X}_{RA}^* , \vec{X}_H^* , \vec{j}_{RA}^* , R) and transducers readouts. The former depends on the geometrical layout of the measurement system and are fixed, whereas the

latter depends upon the particular position of the blade.

For a given set of transducer readouts, the procedure employed to solve the equation is based on a Newton-Raphson method; starting from an initial guess, the method proceeds by inverting the Jacobian matrix ($J_{\vec{\phi}}$) until the value of the objective function $\vec{\phi}$ is below a given tolerance.

The following scheme block depicts the iterative procedure for the blade angles reconstruction:

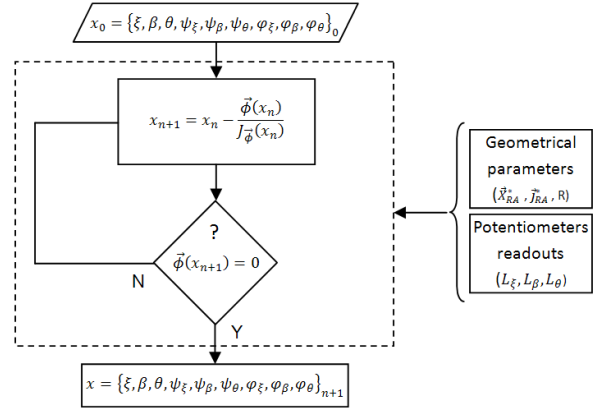


Figure 9: Iterative procedure scheme

5 ON-GROUND CALIBRATION OF THE SYSTEM

In order to process the transducers acquisition and evaluate the blade angles, it is necessary to calibrate the acquisition system. The calibration is necessary because the transducer readouts (s^{POT}) is not directly the total length (L) of the cable from the pulleys centre \vec{X}_{RA}^* to the cable end \vec{X}_E^* (which appears in the Eq. 4-9), but it is a relative measure which zero depends on the calibration of the potentiometer. Therefore the total length can be expressed as:

$$\begin{cases} L_\xi = s_\xi^{POT} + \Delta L_\xi \\ L_\beta = s_\beta^{POT} + \Delta L_\beta \\ L_\theta = s_\theta^{POT} + \Delta L_\theta \end{cases} \quad \text{Eq. 5-1}$$

The three offsets ΔL (one for each potentiometer) are the output of the calibration procedure.

The data necessary for the calibration are obtained by means of an on-ground activity. The test is performed by measuring the blade angles while enforcing different pitch angles to the blades by means of the collective flight controls.

The pitch and flap angles have been evaluated through a clinometer mounted on the blade.

The lag angle has been indirectly measured through a plumb line by converting the arch described on the ground to an equivalent lag angle. Notice that this procedure can estimate only the relative angle with

respect to the initial position of the blade, hence an offset in the lag angle output shall be expected.

Since the total lengths of the cables L_{ξ} , L_{β} , L_{θ} are unknown (see Eq. 5-1), then for any set of offsets $(\Delta L_{\xi}, \Delta L_{\beta}, \Delta L_{\theta})$ a set of blade angles is obtained. The calibration problem consists in evaluating the optimum set of cable offsets, such that the error between the reconstructed blade angles and those experimentally measured is minimized:

$$\text{find } (\Delta L) \rightarrow \min(\bar{\varepsilon}(\xi, \beta, \theta, \xi_{EXP}, \beta_{EXP}, \theta_{EXP}; \Delta L_{\xi}, \Delta L_{\beta}, \Delta L_{\theta})) \quad \text{Eq. 5-2}$$

$\bar{\varepsilon}(\dots)$ is the function that averages the blade angles error evaluated over the set of tested conditions.

In Figure 10, the experimental (red squares) vs. reconstructed (blue circles) normalized blade angles, associated to the calibration test conditions are reported:

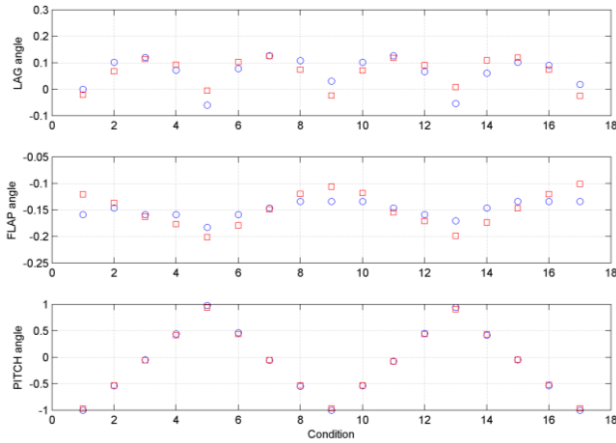


Figure 10: Experimental (red squares) vs. reconstructed blade angles (blue circles) on calibration tests

The accuracy obtained in this calibration, performed during an "on field test" depends on the errors committed in measuring the blade angles by means of the clinometer and the plumb line.

Such errors depend on: i) the misalignment of the mast axes with respect to the ground, ii) a small rigid rotation of the rotor with respect to the mast axis during commands input and iii) other systematic and/or casual errors.

The reconstructed angles for the same command inputs show a good repeatability, with angle differences smaller than 0.1° , lower than the accuracies of the calibration test.

6 FLIGHT ACTIVITY AND VALIDATION

Besides the analytical validation, it is crucial to experimentally verify the blade angles reconstruction procedure.

Below, an example of the in-flight blade angle reconstruction is reported; the flight condition

considered is a forward flight. In Figure 11, the upper axes show the readouts of the three transducers (s^{POT}), the lower axes show the reconstruction of the (normalized) lag, flap, and pitch blade angles.

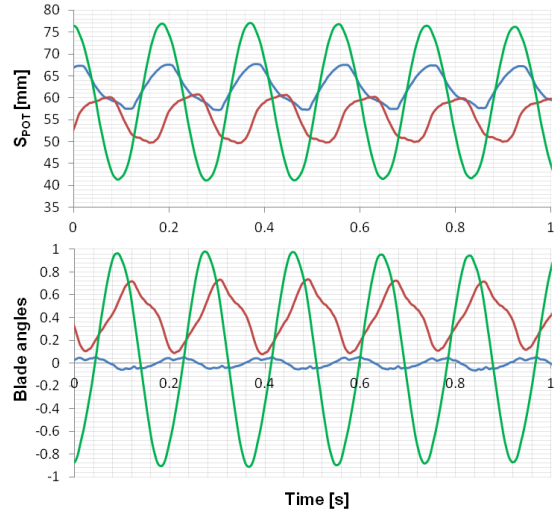


Figure 11: Blade angles reconstruction example (lag transducer/lag angle in blue, flap transducer/flap angle in red, pitch transducer/pitch angle in green)

The readouts of the transducer are smooth and characterized by a very low level of noise that allows a high accuracy of the blade angles reconstruction; this is a peculiarity of the new string potentiometer architecture. In the following, the validation of the blade angles reconstruction is regarded. This is done by correlating the in-flight reconstructed blade angles with other parameters that are in relation with these entities. These relations arise both from the rotor theory and from kinematic considerations. The following paragraphs show the correlation between the reconstructed blade angles and other significant main rotor parameters by processing a subset of level flight conditions.

6.1 Pitch Correlation

The correlation considered is between the MR collective and cyclic commands (in terms of commanded blade pitch angle) and the corresponding reconstructed collective and cyclic pitch blade angle. The collective command is compared to the static value of the reconstructed pitch angle, whereas the cyclic command is compared to the lateral (sine) and (cosine) longitudinal components of the 1/rev pitch angle. The commanded blade pitch angle is evaluated by means of the command chain calibration that relates the collective and cyclic sticks position to the collective and cyclic blade pitch angle.

Notice that the reconstructed pitch blade angle differs from the commanded due to kinematic coupling of the pitch with the flap angle. Therefore in

order to correlate the pitch, the collective and cyclic commands are compared to the reconstructed collective (θ_{COLL}^{REC}) and cyclic commands ($\theta_{LAT}^{REC}, \theta_{LONG}^{REC}$), that can be evaluated starting from the reconstructed pitch and flap angle as follows:

$$\begin{aligned}\theta_{COLL}^{REC} &= \theta_0^{REC} + \tan(\delta_3) \beta_0^{REC} \\ \theta_{LAT}^{REC} &= \theta_{1c}^{REC} + \tan(\delta_3) \beta_{1c}^{REC} \\ \theta_{LONG}^{REC} &= \theta_{1s}^{REC} + \tan(\delta_3) \beta_{1s}^{REC}\end{aligned}\quad \text{Eq. 6-1}$$

In Figure 12, the correlation between the collective pitch command (θ_{COLL}) and the reconstructed collective pitch command (θ_{COLL}^{REC}) is reported; the linear interpolation of the data is also shown. In the next figures the quantities are normalized to the maximum range of the flight command chain.

In Figure 13 and Figure 14 the correlations between the longitudinal and lateral cyclic pitch command ($\theta_{LAT}, \theta_{LONG}$) and the reconstructed longitudinal and lateral cyclic pitch command ($\theta_{LAT}^{REC}, \theta_{LONG}^{REC}$) are shown.

The figures show a good agreement between the pitch command and the reconstructed pitch command, both in terms of collective and cyclic.

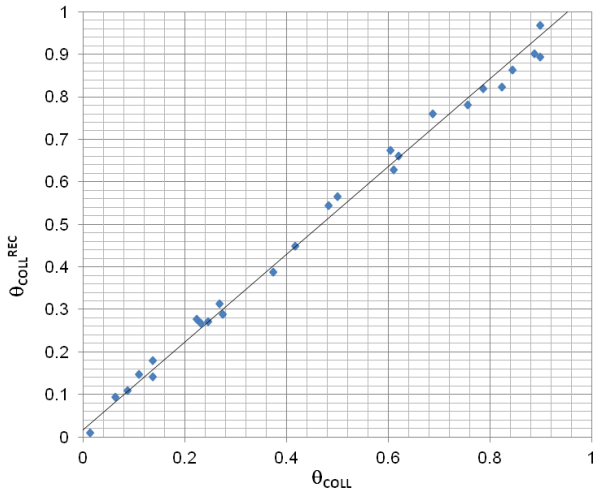


Figure 12: Collective blade angle correlation

6.2 Lag correlation

In order to analyze the correlation of the reconstructed blade lag angle, the relation between the main rotor static torque and the static lag angle is considered.

The relation arises from the dynamic equilibrium between the centrifugal force and the drag that generates opposite moments at the blade hinge. The equation for an articulated rotor with a lag spring (see Ref. [2]) can be evaluated as follows:

$$\xi_0^{TH} = \frac{TQ + N_b(e S_b \Omega^2 lcf + K_b)}{N_b(e S_b \Omega^2 + K_b)} \quad \text{Eq. 6-2}$$

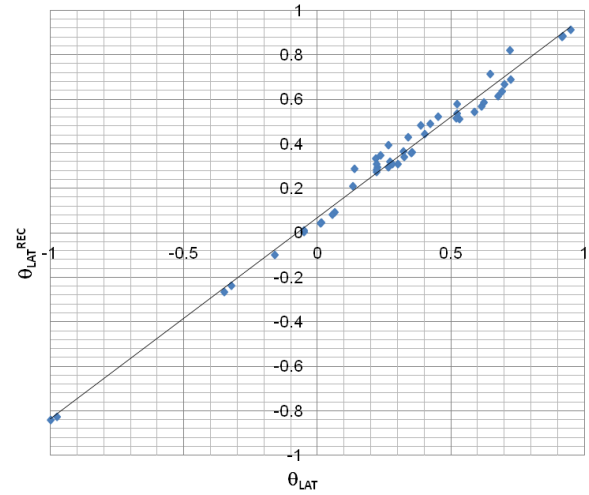


Figure 13: Lateral cyclic blade angle correlation

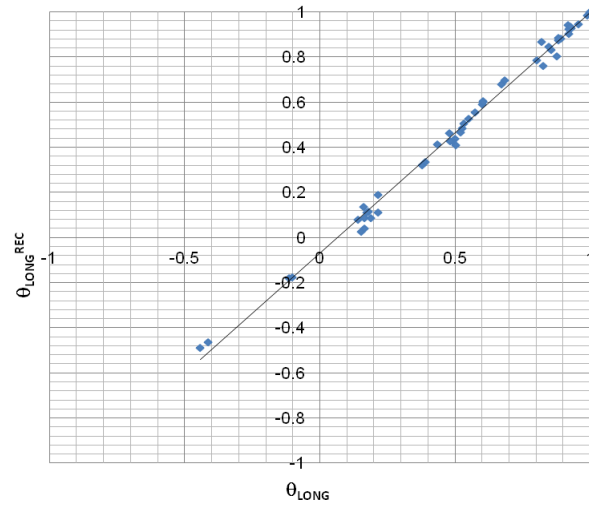


Figure 14: Longitudinal cyclic blade angle correlation

Where TQ is the Main Rotor torque recorded in flight, Ω is the rotor speed, N_b is the number of blades, e is the hinge offset, S_b is the blade static moment, lcf is the tangent of the ratio between the torque offset and the hinge offset, K_b is the damper rotational stiffness.

In Figure 15, the blue squares shows the correlation between the MR torque and the reconstructed static lag blade angle (ξ_0^{REC}), the red squares shows the theoretical static lag angle (ξ_0^{TH}) obtained via Eq. 6-2. Both axes are normalized, the abscissa with the torque corresponding to the maximum continuous power and the ordinate with the maximum static lag angle recorded during the conditions considered.

As showed in Figure 15, the correlation is good in terms of slope, whereas the offset between the two data sets (reconstructed and theoretical) is due to the fact that the system calibration has been

performed in terms of relative lag angle due to difficulty in evaluating its absolute value during the test.

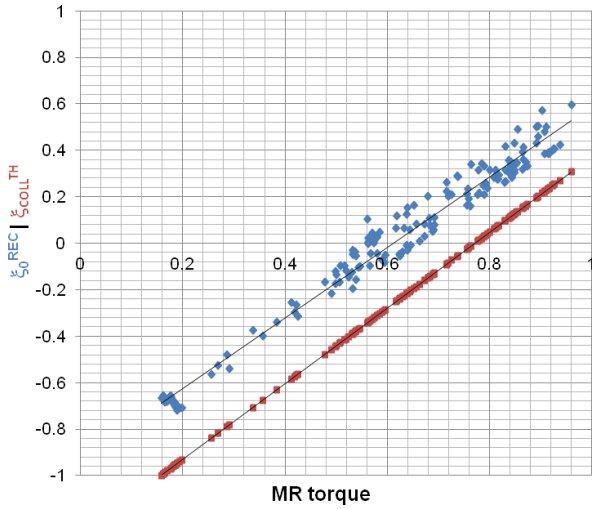


Figure 15: Static lag blade angle vs. MR torque

The estimate of the accuracy in the reconstruction of the lag angle between the slopes of the linear interpolation is good.

6.3 Flap Correlation

In order to correlate the reconstructed flap blade angle, the relation between the cyclic flap angle and the control moment is considered.

In first approximation, for an articulated rotor in a level flight condition, the theoretical relation between the static control moment at the hub centre (CM) and the 1/rev flap blade angle can be written as follows:

$$CM = \left(\frac{N_b}{2} e S_b \Omega^2 + K_f \right) \beta_1 \quad \text{Eq. 6-3}$$

On the other hand, the amplitude of the 1/rev mast bending (MB1), measured on the helicopter, is close to the value of the static control moment. This is true neglecting in first approximation the mast bending effect due to the in-plane shears at the hub center.

In Figure 16, the control moment (CM, red squares) and the 1/rev amplitude of the mast bending (MB1, blue squares) are reported as function of the amplitude of the 1/rev reconstructed flap blade angle (β_1^{REC}). Both abscissa and ordinate are normalized.

The figure shows a good agreement between the theoretical control moment and the acquired mast bending.

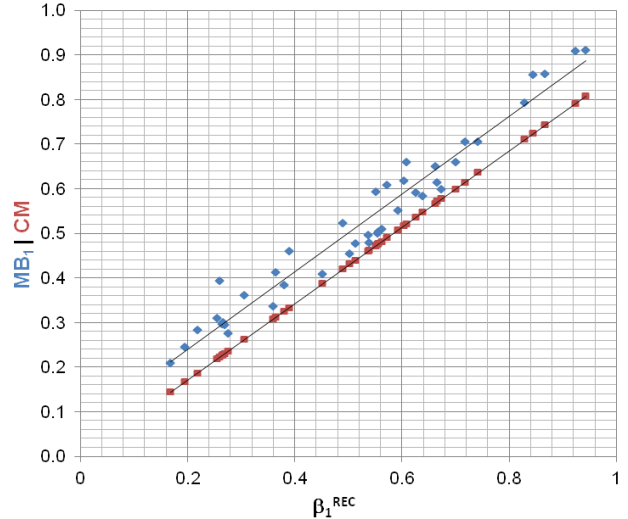


Figure 16: CM, MB₁ vs. 1/rev flap blade angle

6.4 Adjacent Blade Correlation

Two different blade angles reconstruction systems are mounted on two adjacent blades, the white and yellow blades (see Figure 17), where the white blade comes first following the rotor direction of rotation:

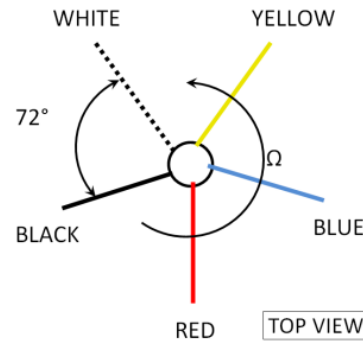


Figure 17: MR blade color scheme

Thanks to this redundancy, it is possible to compare the angles of two blades in order to verify the reliability of the system. In the following, a forward flight condition is analyzed and the results obtained with the two systems are compared.

In Figure 18 the time histories of (normalized) lag, flap and pitch reconstructed with the two systems are reported.

The time histories are very similar in shape and amplitude; the angles that refers to the blade that come first (white blade, dotted lines) are in advance as expected.

The differences between pitch and flap reconstructions of two subsequent blades are low, which is a very good outcome.

7.1 Damper Rotation Correlation

In this paragraph the correlation between the reconstructed damper rotation and the damper rotation acquired in flight, is shown.

In the figures below, the static and the 1/rev magnitude of the damper rotation are reported. On the abscissa, the (normalized) damper rotation acquired on the instrumented damper, on the ordinate the (normalized) reconstructed damper rotation.

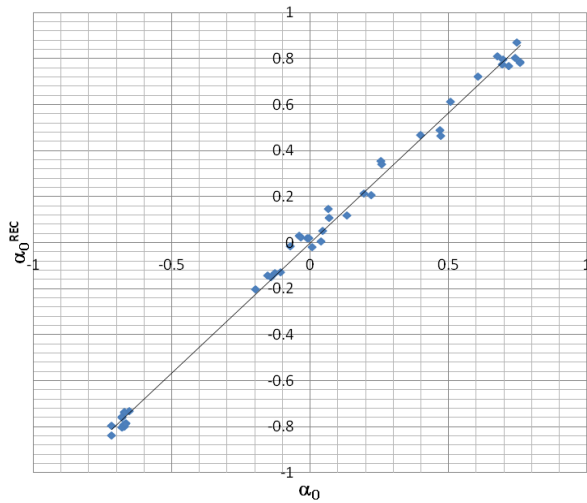


Figure 20: Static damper rotation correlation

The figures show a good agreement between the acquired and reconstructed damper rotation, both in terms of static and 1/rev amplitude.

This result is remarkable, since the damper rotation depends on six blade angles of two different blade reconstruction systems.

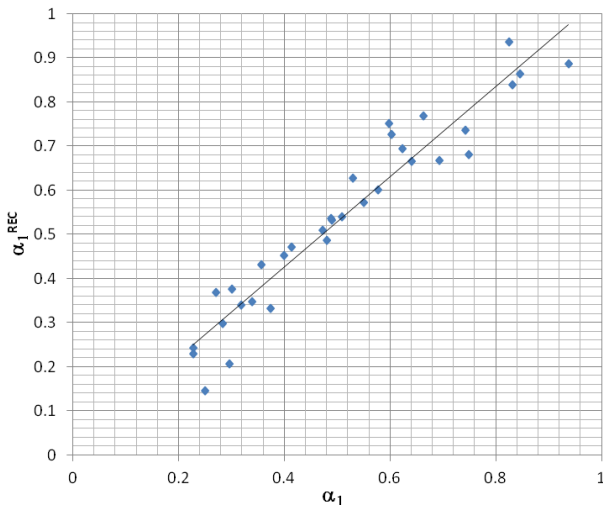


Figure 21: 1/rev damper rotation correlation

8 COMPUTATION OF ROD-END BEARING ROTATION

The evaluation of the bearing rod-ends rotations is possible once the two sets of adjacent blade angles (white and yellow blades, see Figure 19) and the damper rotation are known.

The rotation considered are the following (with this sequence): torsion, cocking in-plane (cocking 1), cocking out-of-plane (cocking 2). Both the inboard and outboard bearings rotations are evaluated.

The torsion is performed around an axis normal to the rod-end (\vec{n}_{TOR}^{DL} in Figure 22), the cocking out-of-plane is performed around an axis directed as the damper link axis (\vec{n}_{CK1}^{DL}) and the cocking in-plane is performed around an axis orthogonal to the previous (\vec{n}_{CK2}^{DL}) as to create a right-handed Cartesian coordinate system.

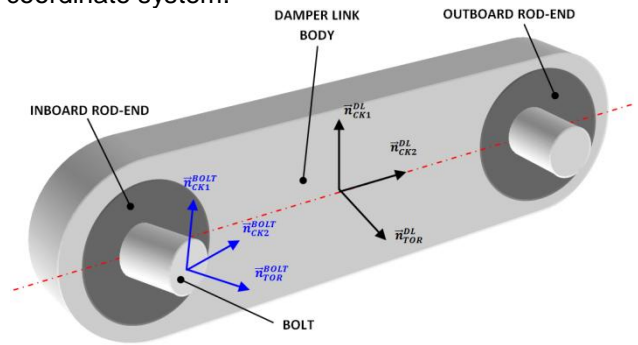


Figure 22: Damper link rod-end simplified scheme

The detailed equation used to evaluate the rod-ends rotation is not presented here. The problem consists in a inverse kinematic problem with finite rotations and only a hint of the solution is discussed.

The problem is: given two sets of Cartesian coordinate systems, one attached to the damper link body and the other one attached to the rod-end bolt (outboard and inboard), evaluates the rotations that superpose the former to the latter with a given sequence of rotations.

Notice that the inboard rod-end coordinate system is attached to a bolt that rotates with the white blade, whereas the outboard coordinate system is attached to the damper which in turn is attached to the yellow blade. The damper link coordinate system rotates in such a way to satisfy the congruence of the damper link length.

The solution in terms of rod-end bearing rotation is obtained through a MATLAB code that implements the kinematic equation discussed above.

8.1 Rod-end rotation validation

The rod-end bearing rotation validation with in-flight correlation is not possible, due to the absence of a parameter related with these entities.

The validation of the rod-end bearing rotation has been performed through an ADAMS model. The

model describes the kinematic of inter-blade main rotor, comprehensive of damper and damper link.

In the following figure, the (normalized) inboard rod-end rotations obtained with the rod-end bearing reconstruction and via the ADAMS model are reported.

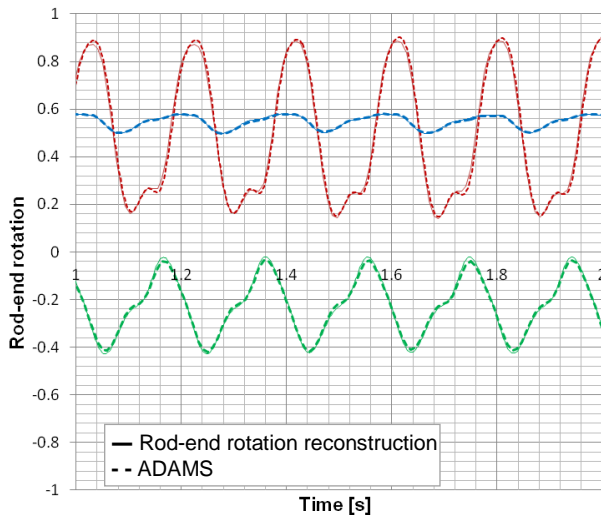


Figure 23: Rod-end bearings rotation validation. The solid line (—) shows the rod-end reconstruction, the dotted lines (--) the ADAMS solution (torsion in red, cocking in-plane in blue, cocking 2 in green).

The two solutions are almost exactly superposed; small differences are due to different setup of the numerical convergence criteria.

9 CONCLUSIONS

The application of a new concept of blade motion measurement system applied to a recently developed main rotor inter-blade architecture has been presented. This new system employs string potentiometer sensors which have been selected in order to enhance installation easiness and flexibility as well as in order to comply with compactness requirements.

The paper describes all the measurement system design, starting from the early hardware design and through dedicated software implementation, up to the final phases of system calibration, flight data processing and correlation.

Results about blade pitch, lag and flap angle reconstructions have been provided in terms of time histories at two consecutive blades; in addition, a rigid modeling of the rotor inter-blade kinematics and the subsequent process validation in terms of damper rotation, both measured in flight and analytically reconstructed, has been presented.

Starting from these results, which provide a solid basis to extend the investigation about rotor in-flight dynamic behavior, the evaluation of the damper link rod-end rotations has been presented.

The results obtained by means of this new measurement system are reliable, both in terms of accuracy angles reconstruction (blade angle, damper angle and rod-end bearing angles) and in terms of reliability, compactness and improvements with respect to previous designs.

The system flew on the AW169 prototype for over than 100 flight hours without technical issues and providing high accuracy of its measures. Moreover, the good reconstruction of damper motions starting from measurements on two consecutive blades can be considered a significant achievement, validating the entire process and providing a solid basis to infer rod-end rotations from the reconstructed kinematics.

The advantage of this new concept of measurement system is the possibility to easily retrofit it on existing rotors with minimum design impact and optimization effort. Possible improvements are related to the on-ground calibration procedure that could represent the core of a future continuation work.

10 COPYRIGHT STATEMENT

The authors confirm that they, and/or their company or organization, hold copyright on all of the original material included in this paper. The authors also confirm that they have obtained permission, from the copyright holder of any third party material included in this paper, to publish it as part of their paper. The authors confirm that they give permission, or have obtained permission from the copyright holder of this paper, for the publication and distribution of this paper as part of the ERF2014 proceedings or as individual offprints from the proceedings and for inclusion in a freely accessible web-based repository.

11 REFERENCES

- [1] Bielawa, Richard L., "Rotary wing structural dynamics & aeroelasticity" Second Edition, AIAA, 2002.
- [2] Wayne Johnson, Helicopter, Dover Publications
- [3] Attilio Colombo, Alessandro Locatelli, "Measuring blade angular motions: a kinematical approach", ERF 2004